Magnetoresistance in a High Mobility Two-Dimensional Electron System as a Function of Sample Geometry

2013 J. Phys.: Conf. Ser. 456 012003

(http://iopscience.iop.org/1742-6596/456/1/012003)

Journal of Physics: Conference Series **456** (2013) 012003 doi:10.1088/1742-6596/456/1/012003

Magnetoresistance in a High Mobility Two-Dimensional Electron System as a Function of Sample Geometry

L. Bockhorn[1], A. Hodaei[1], D. Schuh[2], W. Wegscheider[3], R. J. Haug[1]

[1] Institut für Festkörperphysik, Leibniz Universität Hannover, D-30167 Hannover, Germany
[2] Institut für Experimentelle und Angewandte Physik, Universität Regensburg, D-93053 Regensburg, Germany
[3] Laboratory for Solid State Physics, ETH Zürich, CH-8093 Zürich, Switzerland

E-mail: bockhorn@nano.uni-hannover.de

Abstract. In a high mobility two-dimensional electron gas (2DEG) realized in a GaAs / $Al_{0.3}Ga_{0.7}As$ quantum well we observe changes in the Shubnikov-de Haas oscillations (SdHO) and in the Hall resistance for different sample geometries. We observe for each sample geometry a strong negative magnetoresistance around zero magnetic field which consists of a peak around zero magnetic field and of a huge magnetoresistance at larger fields. The peak around zero magnetic field is left unchanged for different geometries.

1. Introduction

The increased mobility of the two-dimensional electron gas (2DEG) has allowed not only the observation of the fractional quantum Hall effect (FQHE)[1],[2] at low magnetic fields but also many new effects. While the mobility and quality of the samples increases the electron-electron interaction becomes more important for the magnetotransport at low magnetic fields. One effect influenced by the electron-electron interaction is the observation of a strong negative magnetoresistance around zero magnetic field. This strong negative magnetoresistance consists of a peak around zero magnetic field and of a huge magnetoresistance at larger magnetic fields, both effects show a parabolic field dependence [3].

We study here the influence of the sample geometry on the strong negative magnetoresistance, whereas in previous measurements the temperature dependence and the electron density dependence of the strong negative magnetoresistance was analyzed [3, 4].

2. Sample Information

Our samples were cleaved from a wafer of a high-mobility $GaAs/Al_{0.3}Ga_{0.7}As$ two-dimensional electron system (2DES) grown by molecular-beam epitaxy. The quantum well has a width of 30 nm and is Si-doped from both sides. The 2DES is located 150 nm beneath the surface and has an electron density of $n_e = 3.2 \cdot 10^{11}$ cm^{-2} and a mobility of $\mu_e = 11.9 \cdot 10^6$ cm^2/Vs. The different geometries were defined by photolithography and by wet etching. Our measurements were performed in a dilution refrigerator with a base temperature of 20 mK. The magnetotransport measurements were carried out by using low-frequency (13 Hz) lock-in technique.

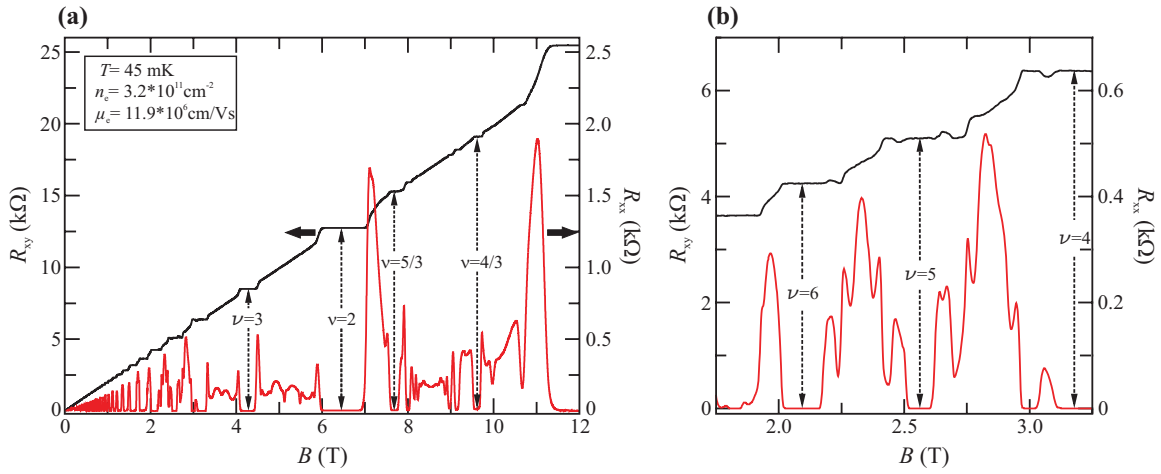

Figure 1. **(a)** The Hall resistance R_{xy} and the longitudinal resistance R_{xx} vs. the magnetic field B. **(b)** Observation of the reentrant integer quantum Hall effect (RIQHE).

The different geometries produced from the high-mobility 2DES will be discussed in the following section. In the next sections we present our magnetotransport measurements for a Hall geometry, especially for the magnetic field range of the strong negative magnetoresistance. The second geometry consists of four Hall bars with different length-to-width ratios.

3. Hall Geometry

The Hall bars have a total length of 1.2 mm, a width of $w = 200$ μm and a potential probe spacing of $l = 300$ μm. Different ungated and gated samples were used for the magnetotransport measurements. In case of the gated sample there is an additional layer of 600nm PMMA between the Hall bar and the metallic topgate to avoid leakage current.

Figure 1 (a) shows the Hall resistance R_{xy} and the longitudinal resistance R_{xx} vs. magnetic field B to demonstrate the quality of our samples. The longitudinal resistance decreases to zero between the integer filling factors $\nu = 4$ and $\nu = 6$ (see Figure 1 (b)), but the corresponding Hall plateaus are quantized at integer values, e.g. at $B = 3.0$ T. This phenomenon is called the reentrant integer quantum Hall effect (RIQHE) and is often observed in high mobility samples [5, 6]. We observe a clear minimum in the longitudinal resistance for the filling factor $\nu = 5/2$ at $B = 5.1$ T. The filling factor $\nu = 5/2$ is only observed in high mobility samples and low temperatures. Also a series of different fractional quantum Hall states is observed for filling factors $\nu < 2$. The fractional filling factors $\nu = 5/3$ and $\nu = 4/3$ are marked in Figure 1 (a).

We observe a strong negative magnetoresistance around zero magnetic field which can be divided into two regions (see Figure 2). The two regions consist of a peak around zero magnetic field and of a huge magnetoresistance at larger fields.

3.1. ***Peak around zero magnetic field***

The longitudinal resistivity vs. the magnetic field is shown in Figure 2. The peak around zero magnetic field is fitted to a parabolic magnetic field dependence. In previous experiments we observed that the curvature of the peak is left unchanged by increasing the temperature to 0.8 K [3]. This temperature independence of the peak is a sign for the absence of weak localization. Also for different electron densities the curvature of the peak is left unchanged. We assume according to Mirlin *et al.* [7] that the peak is induced by an interplay of smooth disorder and rare strong scatteres.

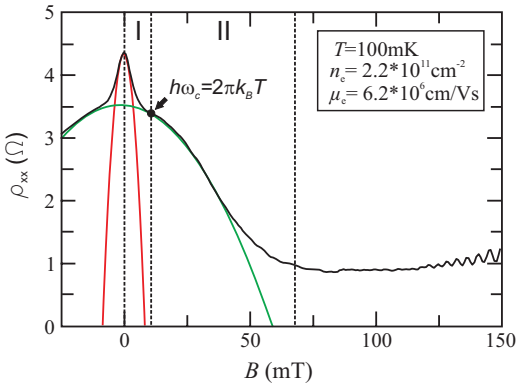

Figure 2. The longitudinal resistivity ρ_{xx} vs. the magnetic field B. The strong negative magnetoresistance is divided into two sections.

3.2. ***Huge Magnetoresistance***

Previous publications reported on a strong negative magnetoresistance, which vanished by increasing the temperature [3, 4]. The huge magnetoresistance in Figure 2 depends not only strongly on the temperature, it depends also strongly on the electron density and it becomes more pronounced by decreasing the electron density. Also the huge magnetoresistance is fitted by a parabolic magnetic field dependence.

We examine the electron-electron interaction correction to the conductivity in the situation of a long-range fluctuation potential and in the regime of ballistic transport [8]-[11] to describe the huge magnetoresistance. In accordance with Gornyi *et al.* [11] we assume a model of mixed disorder to fit the huge magnetoresistance. The electron interaction induced correction to the conductivity considering the model of mixed disorder is expressed by

$$\rho_{xx} = \rho_0 - \rho_0 \, \frac{c_0}{n_e^2 \, \pi \, h} \sqrt{\frac{\hbar}{T\tau \, k_B}} \cdot \alpha \cdot \; B^2 \tag{1}$$

with $c_0 = 0.276$. ρ_0 is the longitudinal resistivity at zero magnetic field, n_e is the electron density, τ is the transport scattering time, T is the electron temperature and k_B is the Boltzmann constant. The factor α is in accordance with Gornyi *et al.* [11] expressed by $\alpha = 4(\tau_{sm}/\tau)^{-1/2}$ with $\tau_{sm} = (k_F d)^2 \tau_q$ depending on the quantum scattering time τ_q. The expected temperature dependence of $T^{-1/2}$ from the electron interaction correction to the conductivity is observed for temperatures below 400 mK. Above 400 mK the curvature is approximately proportional to T^{-1} as long as the huge magnetoresistance is observable.

We observed a discrepancy between our measurement and theory. The factor α determined from the curvature of the huge magnetoresistance is larger than the expected value. A possible origin of this discrepancy between theory and experiment is that the quantum scattering time τ_q is dominated by smooth disorder. The influence of the strong scatterers should also be considered in the quantum scattering time because of the description of the peak around zero magnetic field.

4. Four-in-a-row Hall bar

The second geometry we discuss here consists of four Hall bars with different length-to-width ratios (Figure 3). On the basis of this special geometry we could measure the influence of the geometry on the strong negative magnetoresistance in one cooling cycle. Several samples were produced and measured and all of them showed similar results.

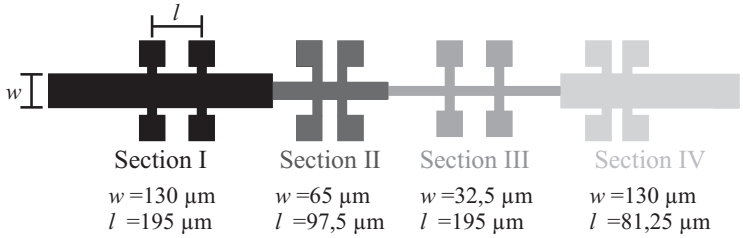

Figure 3. Schema of the four-in-a-row Hall bar. Each section of this geometry has a different width w and a different potential probe spacing l, which are note below the corresponding section.

4.1. ***Geometry Information***

The four-in-a-row Hall bar has a total length of 2.7 mm and is separated into four sections. Each section consists of a Hall bar with a different length-to-width ratio. The first section in Figure 3 has a width of $w = 130$ μm and a potential probe spacing of $l = 195$ μm. The second section has the same length-to-width ratio as section I. The width of the section II is $w = 65$ μm and the potential probe spacing is $l = 97.5$ μm. Section III has the smallest width (w =32.5 μm) and a potential probe spacing of $l = 195$ μm. The section IV has a width of $w = 130$ μm and a potential probe spacing of $l = 82.25$ μm.

Two types of contact geometries are used for the four-in-a-row Hall bar. The potential probe spacing of section I and of section III is large enough to put the ohmic contacts in the middle of the side contact. The situation is changed for the other sections. The potential probe spacing is here too small. The size of the ohmic contacts can't be reduced, so the ohmic contacts are shifted to one side.

4.2. ***Magnetotransport Measurement***

Figure 4 (a) shows the longitudinal resistivity ρ_{xx} and the Hall resistance R_{xy} vs. the magnetic field B for section I of the four-in-a-row Hall bar (red). Also a corresponding measurement of a reference Hall bar (black) is shown. The length-to-width ratio of section I is the same as for the reference Hall bar, so one could expect a similar behavior of the longitudinal resistivity and the Hall resistance. We observe instead that the minima of the longitudinal resistivity of section I increase till filling factor $\nu = 4$, then the longitudinal resistivity decreases. Also the slope of the Hall resistance of section I changes at small magnetic fields and the values of the Hall plateaus are lower than usually. The Hall plateaus are the expected ones only at filling factor $\nu = 4/3$ for magnetic fields $B > 12$ T. This astonishing behavior is observed for each section of the four-in-a-row Hall bar for different samples. The minima of the longitudinal resistivities increase till filling factor $\nu = 4$ for each section of the geometry and then drop to zero. Also the Hall resistances deviate at small magnetic fields for each length-to-width ratio from the linear behavior with magnetic field. The increase of the longitudinal resistivity is stronger for the smallest length-to-width ratio, while the Hall plateaus decrease to lower values for the highest length-to-width ratio.

A possible origin of the unexpected behavior considers charge puddles in the doping layer. The influence of the charge puddles for wide samples is negligible as long the extension of the charge puddles is much smaller than the width of the sample. In the situation of the narrowest section of the four-in-a-row Hall bar the size of the charge puddles could be in the range of the width of the Hall bar and short-circuit the sample in this way. Hence all magnetotransport measurements of this geometry will be influenced by these charge puddles due to the short-circuit in the narrowest part and the interconnection of the whole sample in the quantum Hall

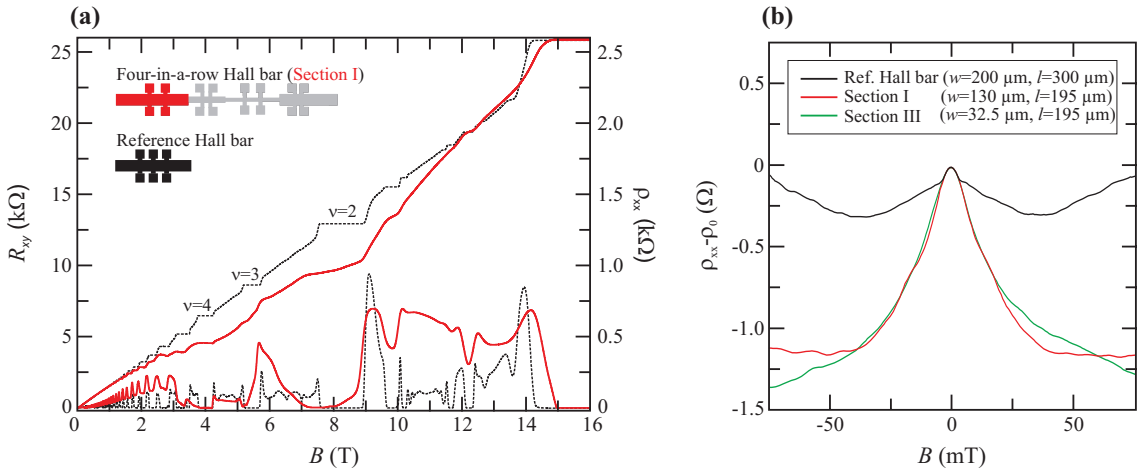

Figure 4. (a) The Hall resistance R_{xy} and the longitudinal resistivity ρ_{xx} of section I vs. the magnetic field B at 45 mK. The dotted line is the corresponding measurement of a reference Hall bar. **(b)** The longitudinal resistivity ρ_{xx} reduced by the corresponding ρ_0 around zero magnetic field for different geometries.

regime.

Figure 4 (b) shows the longitudinal resistivity ρ_{xx} reduced by the corresponding ρ_0 vs. the magnetic field B around zero magnetic field for different geometries. The strong negative magnetoresistance around zero magnetic field is observed for each section of the geometry. The curvature of the peak around zero magnetic field is left unchanged for different length-to-width ratios, while the height of the peak is changed. Differences in the curvature are observed for different sample materials. The situation of the huge magnetoresistance is here more complicated and a conclusion for a geometry dependence is not possible.

5. Conclusion

We observe for each sample geometry a strong negative magnetoresistance around zero magnetic field which consists of a peak around zero magnetic field and of a huge magnetoresistance at larger fields. The huge magnetoresistance depends strongly on temperature and electron density, while the peak around zero magnetic field is left unchanged. The peak around zero is left unchanged also for different geometries.

This work was financially supported by the Cluster of Excellence QUEST.

6. References

[1] D. C. Tsui, H. L. Stormer, and A. C. Gossard, *Phys. Rev. Lett.* **48**, 1559 (1982).
[2] R. B. Laughlin, *Phys. Rev. Lett.* **50**, 1395 (1983).
[3] L. Bockhorn, P. Barthold, D. Schuh, W. Wegscheider, and R. J. Haug, *Phys. Rev. B* **83**, 113301 (2011).
[4] A. T. Hatke, M. A. Zudov, J. L. Reno, L. N. Pfeiffer, and K. W. West, *Phys. Rev. B* **85**, 081304 (2012)
[5] J. P. Eisenstein, *Solid State Commun.* **117**, 123 (2001)
[6] J. P. Eisenstein, K. B. Cooper, L. N. Pfeiffer, and K. W. West *Phys. Rev. Lett.* **88**, 076801 (2002)
[7] A. D. Mirlin, D. G. Polyakov, F. Evers, and P. Wölfle, *Phys. Rev. Lett.* **87**, 126805 (2001).
[8] M. A. Paalanen, D. C. Tsui, and J. C. M. Hwang, *Phys. Rev. Lett.* **51**, 2226 (1983).
[9] I. V. Gornyi and A. D. Mirlin, *Phys. Rev. Lett.* **90**, 076801 (2003).
[10] L. Li, Y. Y. Proskuryakov, A. K. Savchenko, E. H. Linfield, and D. A. Ritchie, *Phys. Rev. Lett.* **90**, 076802 (2003).
[11] I. V. Gornyi and A. D. Mirlin, *Phys. Rev. B* **69**, 045313 (2004).